Desalination 503 (2021) 114929

Contents lists available at ScienceDirect

Desalination

journal homepage: www.elsevier.com/locate/desal

Electrochemical desalination coupled with energy recovery and storage

Umesh Ghimire [a], Mary K. Heili [b], Veera Gnaneswar Gude [a,*]

[a] Richard A Rula School of Civil and Environmental Engineering, Mississippi State University, Mississippi State, MS 39762, USA
[b] Department of Chemistry, University of Wisconsin-Stevens Point, Stevens Point, WI 54481, USA

HIGHLIGHTS

- Zinc|ferricyanide desalination battery provides energy storage for desalination.
- Desalination battery yielded a 30.3% salt removal during a 12-hr discharge.
- 74.2% of energy consumed was recovered by desalination/discharging process.

GRAPHICAL ABSTRACT

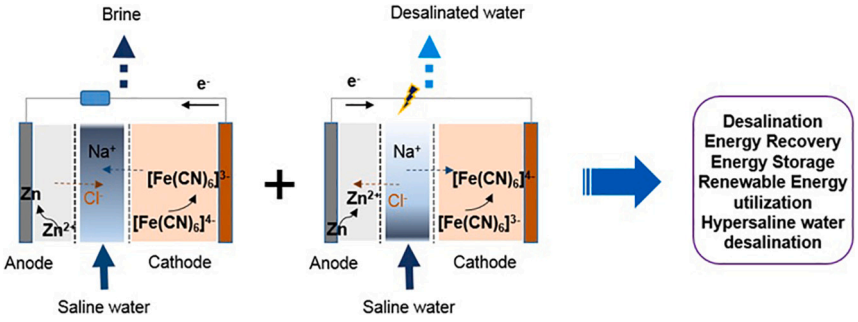

ARTICLE INFO

Keywords:
Desalination battery
Electrochemistry
Energy storage
Electrochemical cells
Saline water

ABSTRACT

This paper presents the performance of a dual-purpose Zinc|ferricyanide desalination battery for simultaneous desalination and energy storage operations. The zinc|ferricyanide battery consists of an anode chamber with a zinc electrode immersed in $ZnCl_2$(aq) electrolyte, a cathode chamber with a graphite electrode and electrolyte solution of $K_3[Fe(CN)_6]$(aq) and $K_4[Fe(CN)_6]$(aq), as well as a middle chamber with saline water to be desalinated. These chambers are separated by anionic and cationic exchange membranes, respectively. A series of experiments were conducted to study the impact of charging and discharging cycles on desalination-salination rates, power storage, and discharge rates at different charging capacities. The electrochemical cell was also characterized in terms of power density and desalination performance under various conditions. Results from this study confirm that the electrochemical battery desalination method has the potential to store energy and the charging-discharging cycles of the battery can provide a mechanism for desalination, which is achieved free of energy consumption. A desalination rate of 30.3% can be achieved during a 12-hr discharge period, which decreased the salinity levels from 41.2 g/L to 28.7 g/L. This result indicates that the process is also suitable for pre-desalination or pretreatment of high saline waters, which is a major challenge for current membrane processes.

1. Introduction

Desalination of saline waters is considered as an energy-demanding process regardless of the technology employed (thermal, membrane, or hybrid technology) [1–3]. The quest for energy-efficient desalination processes is an ongoing endeavor. Predominant desalination

* Corresponding author.
E-mail address: gude@cee.msstate.edu (V.G. Gude).

https://doi.org/10.1016/j.desal.2020.114929
Received 9 September 2020; Received in revised form 17 December 2020; Accepted 20 December 2020

technologies based on thermal and membrane processes are usually faced with energy-, cost-, and process-specific challenges especially when it comes to their applications in high saline water treatment [3,4]. Membrane desalination by reverse osmosis with nanofiltration pretreatment is not a favored approach when the source water total dissolved solids (TDS) concentration is much higher than seawater concentration, i.e., over 35,000 mg/L due to high operating pressures and corresponding electrical energy requirements [2,5]. To address this issue, bioelectrochemical, chemical, and electrochemical energy-based desalination processes are increasingly being considered in recent years due to their potential for providing energy- and resource-efficient treatment of saline and wastewaters either in individual or integrated configurations [6–10]. Recent reports and studies have focused on the need for developing novel membranes to address the energy efficiency, flux, biofouling, and environmental performance of membrane desalination processes through various innovative approaches [11–18]. These include functionalized woven glass fiber membranes [12], sepiolite based nanocomposite membranes [13], innovative bioelectrochemical processes using both anionic and cationic membranes [14,15], incorporation of Ag and Cu nanoparticles or nanorods [16], positively charged nanofiltration membranes [17], and carbon electrodes for enhancing capacitive deionization process [18]. These studies make important contributions to the field, however, energy efficiency and energy recovery with storage should be given a priority to render desalination processes more attractive as 25–40% of water costs are associated with energy costs in desalination processes [19,20].

In general, desalination processes are supported by electricity generated from conventional energy sources although renewable energy penetration is advancing more rapidly in this field [2,21,22]. An energy storage unit may be required for desalination applications due to the large energy demands in the process as well as to store excess energy generated by variant or fluctuating renewable energy generation [23–25]. Electricity and storage costs have also been identified as contributing factors to the product water costs [20,21]. The development of electrochemical batteries can be a solution to both store and supply energy when needed, with potential cost savings of off-site energy generation, and its transportation through grid infrastructure [26–29]. This concept also allows desalination to be carried out spontaneously due to the electrochemical and ionic imbalance caused by charging and discharging cycles which is called electrochemical desalination [30]. Many combinations and configurations of electrochemical cells and desalination configurations can be envisioned [31]. These configurations can be developed by considering different electrode materials, different electrolytes, and different separation and flow configurations. Some of these technologies include capacitive deionization, desalination batteries, and electrodialysis [32–34]. Intercalating electrode materials have also been evaluated to increase salt adsorption capacities [35]. These processes can also be integrated with non-electrochemical processes such as adsorption or oxidation process [36,37] and pressure retarded osmosis [34] to improve desalination capacities, specific ion removal or recovery [38], and specific energy consumption including possible membrane-free desalination [39]. While these processes improved the salt removal efficiency to more than 80%, experimental studies focusing on high salinity waters are still scarce.

In this research, we study the potential of an electrochemical battery for facilitating desalination function during charging and discharging modes, based on an innovative salt separation and energy generation principle reported recently [30]. This method has promising potential and scope for developing an energy-efficient high saline water electrochemical desalination process. Briefly, a zinc chloride and ferricyanide electrochemical desalination battery (EDB) was evaluated. The corresponding oxidation and reduction reactions resulting in the electron flow from anode to the cathode along with their electromotive voltages are shown below. By exploiting the inherent operation principles, a flow battery type configuration can be established between the two redox-active materials.

Anode

$$Zn_{(s)} + 2Cl^{-}_{(aq)} \leftrightarrow ZnCl_{2\,(aq)} + 2e^{-}\ E^{o} = -0.76\ \text{V vs SHE}$$

Cathode

$$2K_3\left[Fe(CN)_6\right]_{(aq)} + 2Na^{+}_{(aq)} + 2e^{-} \leftrightarrow 2K_3Na\left[Fe(CN)_6\right]_{(aq)}\ E^{o} = +0.49\ \text{V vs SHE}$$

Overall

$$Zn_{(s)} + 2K_3\left[Fe(CN)_6\right]_{(aq)} + 2\,NaCl \leftrightarrow ZnCl_{2\,(aq)} + 2K_3Na\left[Fe(CN)_6\right]_{(aq)}\ E^{o} = +1.25\ \text{V}$$

This configuration enables both high-efficiency electrical storage and discharge capacity. When the battery goes through charge and discharges modes, there is a corresponding release and transfer of salt ions through the ion exchange membranes separated by a saline water chamber, thus enabling desalination and salination cycles, respectively as shown in Fig. 1. In this study, the desalination performance of an electrochemical battery is evaluated at different charging and discharging cycles. The effect of charge capacity on desalination performance is evaluated. Power density profiles, discharge capacity, and coulombic efficiency were also analyzed. Results reported from this study provide an improved understanding of the process as the experimental studies are performed at much higher anode, cathode, and desalination volumes. In addition, detailed energy efficiency and salinity removal analyses presented in this manuscript contribute to further development of this novel process.

2. Materials and methods

2.1. Electrochemical desalination battery (EDB) construction

The EBD consisted of three chambers (anode, middle desalination, and cathode), separated by using anionic (AEM) and cationic (CEM) exchange membranes. Anode and desalination compartments were separated by an anion exchange membrane (AMI7001, Membranes International) while cathode and desalination compartments were separated by a cation exchange membrane (CMI7000, Membranes International). To keep the membranes hydrated and expanded, each membrane was pre-conditioned by immersing them in an 85.6 mM NaCl solution at 40 °C for a day and washed with distilled water before their use. The three-compartment EDB was fabricated using Plexiglas (7.2 cm diameter) material with an anode compartment volume (V_{an}) of 30 mL, a cathode compartment volume (V_{ca}) of 30 mL, and a desalination compartment volume (V_{ds}) of 20 mL. Smooth texture solid zinc sheet (with dimensions of 32.3 mm × 22.7 mm × 1 mm for length, width, and thickness, respectively) and graphite electrode (with dimensions of 32.4 mm × 23.2 mm × 2.5 mm for length, width, and thickness, respectively) were used as anode and cathode electrodes, respectively. A titanium wire was used for conducting electricity from the electrodes and for forming a circuit between the electrodes as shown in Fig. S1.

2.2. Catholyte and anolyte solution

The EDB was assembled using the electrolyte solutions and saline water listed in Table 1. 30 mL of $ZnCl_2$ solution (0.2765 M) was

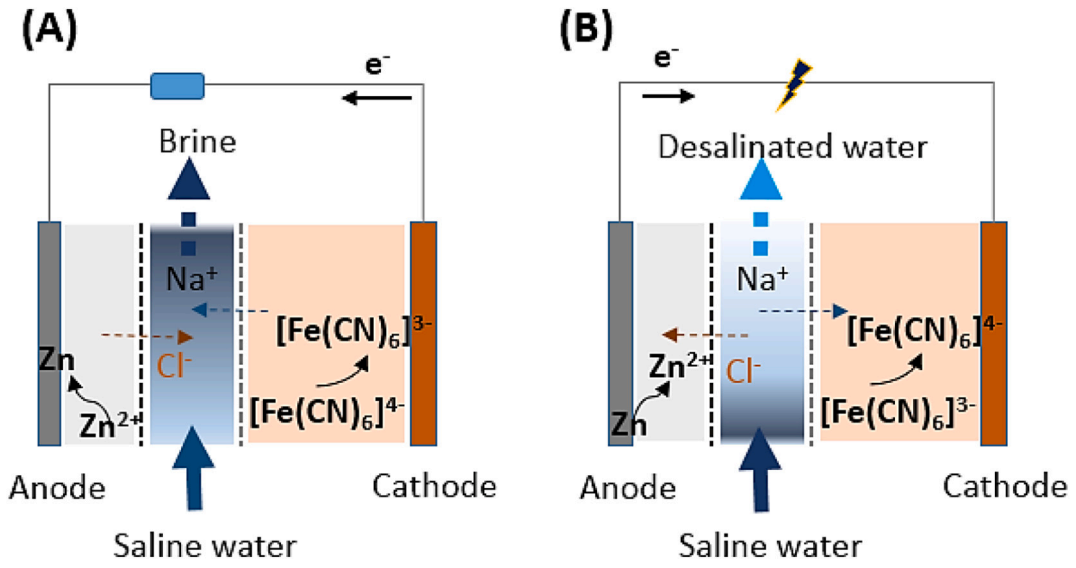

Fig. 1. Electrochemical battery for desalination and salination cycles: (A) charging mode with salination; and (B) discharging mode with desalination.

Table 1
Solute in 100.0 mL of solution.

Solution	Actual mass	Calculated concentration	Initial pH
Saltwater	4.12 g NaCl	41.2 g/L	7.2
Catholyte	9.9375 g $K_3Fe(CN)_6$	0.3018 M	6.6
	12.8654 g $K_4Fe(CN)_6 \cdot 3H_2O$	0.3046 M	
Anolyte	1.0033 g $ZnCl_2$	0.2765 M	5.7

introduced to the cathode chamber with a graphite electrode. The mixture of 30 ml of 0.3046 M $K_4Fe(CN)_6 \cdot 3H_2O$ and 0.3018 M $K_3Fe(CN)_6$ mixture was introduced to the anode chamber with a zinc electrode. The middle chamber of the EDB was fed with 20 mL of 41.2 g/L NaCl solution. It may be possible to use sodium ferricyanide and its oxidation state as catholyte. A comparison was made between the solubilities of potassium ferrocyanide and its oxidized state with sodium ferricyanide and its oxidation state. The solubility of $Na_4[Fe(CN)_6]$ is only 0.56 M in water when compared with the water solubility of $K_4[Fe(CN)_6]$ which is 0.76 M. This presents limited capacity scenario for sodium ferrocyanide and its oxidized state when compared with potassium ferrocyanide and its oxidized state. Limited solubility means that high concentrations of catholyte will not be possible, therefore limiting the battery capacity in redox flow batteries [40]. Moreover, it has been reported that sodium ferricyanide cannot work as cathode material while $Na_4Fe(CN)_6$/NaCl solid solution shows potential for its use [41]. However, it needs to be synthesized through ethanol extraction method at room temperature. This method is not as simple as preparing potassium ferricyanide solution.

2.3. EDB operation and experimental procedure

The three-chambered EDB was fed with anolyte, catholyte, and saline water in the anode, cathode and desalination chambers, respectively. After the introduction of the solutions in respective chambers, the anode and cathode terminals of EDB were connected to the Gamry 1010e potentiostat to perform the charging operation. The EDB was charged for 1 h by applying a constant current of 15 mA (galvanostatic method), desired current density of 2 mA/cm^2 (electrode area 7.5 cm^2). The voltage-current density profile during the 1-hr charging operation of EDB is shown in Fig. S2. After charging it for 1 h, the saline water from the middle chamber was removed. TDS measurement was performed, and replaced the middle chamber with a new batch of saline water. The discharging operation of the cell was performed by dropping the voltage across the load resistor of resistance 68 Ω and the voltage drop across the load resistor was recorded by using a Fluke (287 true Rms) voltmeter at every 5-minute interval. The discharge operation was terminated at a point where the observed voltage is close to zero. However, the cell voltage drop is never truly zero. Therefore, the general rule of thumb followed was that it would be considered zero at a voltage drop of 0.01 V or lower. After the completion of the discharge cycle, the saline water from the middle chamber was removed, TDS was measured and replaced with a new batch of saline water before making it ready for the next charge cycle and the cycle was repeated. The TDS measurement was performed using an EXTECH EC170 salinity meter. Negative numbers regarding TDS values indicate a decrease and positive numbers indicate an increase in salinity. Unless otherwise noted, all salinity readings were taken from a dilution of 2 mL salt solution to 8 mL water. The TDS reading is multiplied by a factor of 5 and the resulting value was reported as the salinity of the sample.

2.4. Calculations

Ohm's law (Eq. (1)) was used to calculate the discharge current.

$$V = I \times R \tag{1}$$

where I is discharge current.

Discharge current density (CD) (A/cm^2) was calculated using Eq. (2):

$$CD = \frac{I}{A} \tag{2}$$

where A = electrode area = 7.5 cm^2

Power density (PD) (W/cm^2) was calculated using Eq. (3):

$$PD = CD \times V \tag{3}$$

Salt removal was calculated using Eq. (4):

$$\%\text{salt removal} = \frac{\text{Initial TDS} - \text{Final TDS}}{\text{Initial TDS}} \times 100\% \tag{4}$$

Discharge and Charge capacities were calculated by Eqs. (5) and (6):

$$\text{Discharge capacity } \left(\text{Ah}/\text{cm}^2\right) = CD \times T_d \tag{5}$$

where T_d = discharge cycle time in hours

$$\text{Charge capacity } \left(\text{Ah}/\text{cm}^2\right) = \text{charge current density} \times T_c \tag{6}$$

T_c = charge cycle time, in hours

Columbic efficiency (CE) was calculated using Eq. (7):

$$\text{Columbic efficiency (CE)} = \frac{\text{discharge capacity}}{\text{charge capacity}} \quad (7)$$

3. Results and discussion

The design and experimental results of electrochemical zinc|ferricyanide desalination battery (EDB) are presented in this section.

3.1. Power density profile during charging and discharging

This EDB configuration enables electrical energy storage along with the separation of salts from saline water. It is operated between charge and discharge half-cycles of the EDB battery. The discharge-half cycle initiates the removal of NaCl from the middle desalination chamber in which the zinc anode is oxidized to Zn^{2+} ions (in anode chamber) and draws the Cl^- from the desalination chamber to the anode chamber through the anion exchange membrane (AEM). At the same time, ferricyanide is reduced to ferrocyanide in the cathode chamber allowing Na^+ to migrate towards the cathode chamber through the cation exchange membrane (CEM). The charging and discharging current density profiles of the EDB are presented in Fig. 2. The EDB was charged for 1 h by applying a constant current of 15 mA (galvanostatic method) at a desired current density of 2 mA/cm^2 (electrode area 7.5 cm^2) and was discharged by connecting a resistor of resistance 68 Ω until the voltage across it reached below 0.01 V. The average discharging cycle period for each cycle was recorded as 1.5 ± 0.15 h (Fig. 3). The average maximum power density generated by the EDB during the discharge process at 68 Ω of load resistor was 1.41 ± 0.06 mW/cm^2, which is about 50% lower than that of the applied power density during the charging process.

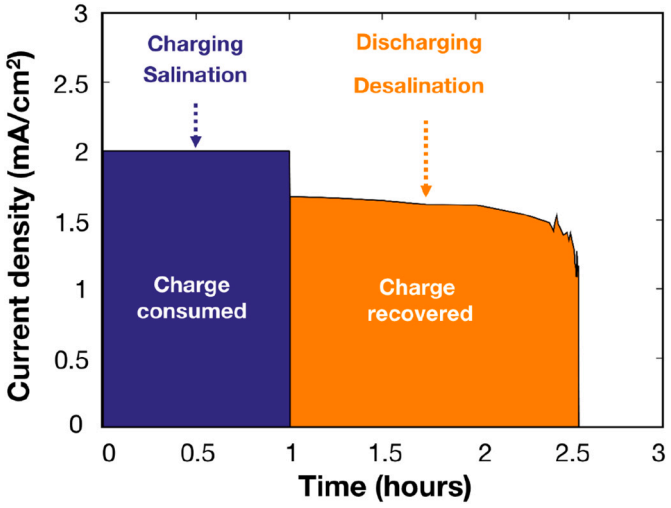

Fig. 3. The current density applied to EDB during the charging process and current density produced by EBD during the discharging process with time.

The rise and fall of salinity of the saline water in the desalination chamber were observed during the charging and discharging process, respectively. During 1 h of charging operation, the average salinity of the desalination chamber was increased from 41.2 g/L to 42.78 ± 0.1 g/L (an increase of 3.8%) while during discharging operation the average salinity of the desalination chamber decreased from 41.2 g/L to 38.85 ± 0.7 g/L, which is about 6.5% reduction in salinity (Fig. 2B). The higher desalination rate than that of the salination rate was as expected because of the longer discharge cycle than that of the charge cycle. Furthermore, to analyze the effect of charging time in the performance of EDB, the

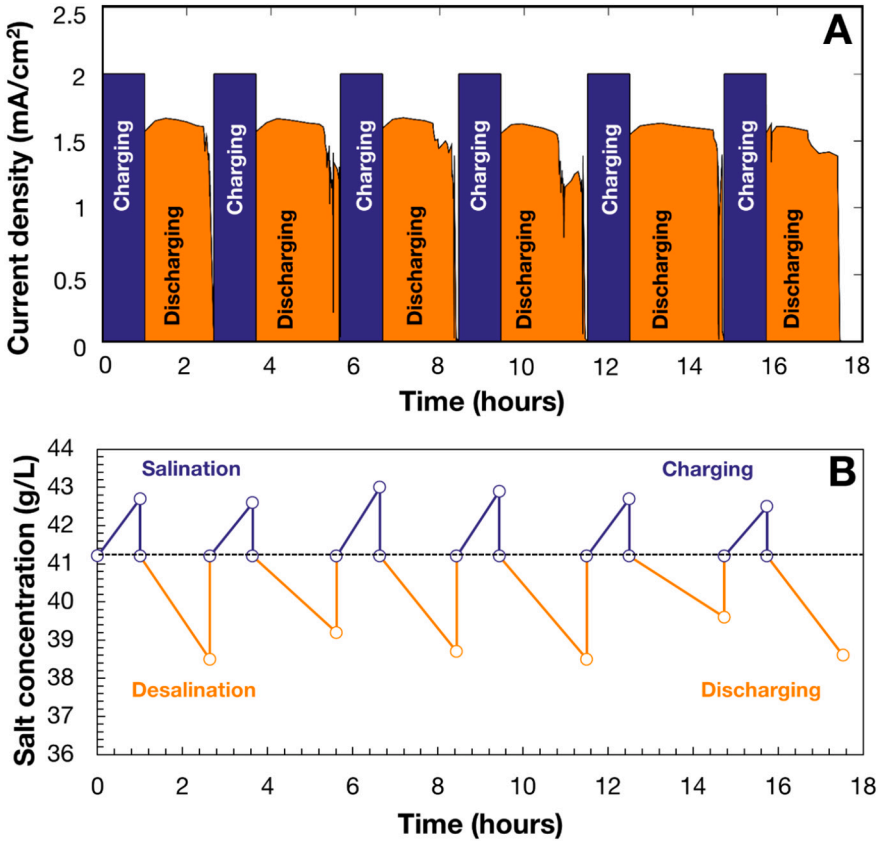

Fig. 2. (A) Current density vs time for the number of charging and discharging cycles of a cell and (B) salinity profiles in the desalination chamber during charging and discharging periods of the EDB with a load resistor of 68 Ω.

charging time of EDB was increased to 4 and 8 h. The results show that an increase in charging time increased the salinity of the saline water in the desalination chamber. When EDB was charged for 4 h, the salinity of the desalination chamber was increased to 16.5%, and charging EDB for 8 h increased the salinity of the desalination chamber to 27.1% (Fig. 4). Moreover, the discharging cycle period (at a load of 68 Ω) and desalination rate of EDB were found to be influenced by the charging period. The EDB was charged for 4 h and was discharged through a 68 Ω resistor. The discharge cycle has lasted for 11 h and the salinity of the desalination chamber decreased from 41.2 g/L to 30.8 g/L (25.2% decrease) (Fig. 4). Similarly, the EDB was charged for 8 h and discharged through a 68 Ω resistor but the discharge cycle has only lasted about 12 h with a decrease in salinity of the desalination chamber from 41.2 g/L to 28.7 g/L (30.3% salinity removal) (Fig. 4). The salination and desalination rates increased with the charging periods in different electrochemical desalination cell experiments. An increase in the charging time from 6 h to 9 h increased the desalination rate from 40% to 60% in a zinc|ferricyanide hybrid flow battery [30]. However, the experimental setup in their study was 5–10 times smaller than the present study. Results from this experiment confirm that the desalination rate may be affected by variations in electrochemical cell configuration, reactor dimensions, and other mass transfer related limitations.

3.2. Polarization and charging/discharging capacity for each cycle

The electrochemical behavior of the EDB was studied by analyzing polarization curves and power density profiles (Fig. 5A). The polarization test was conducted by using a constant resistance discharge method where different resistors (10 Ω to 20,000 Ω) were applied to the EBD and by measuring the resulting voltages and current values. The power density profile was calculated using a polarization curve. This test was performed during the 4th discharging cycle. The results showed that the maximum power density of 1.23 mW/cm^2 was produced at an external resistance of 50 Ω, which implies that the maximum power point has occurred at a load resistor of 50 Ω. Fig. 5B shows the performance of the EDB reporting the charging and discharging capacity over 6 cycles of operation. The charging capacity of the EBD was analyzed based on 1 h of charging period and the discharging capacity of the EBD was calculated based on the same discharging period (1 h). Results showed that during the charging (salination) and discharging (desalination) process, the EDB maintained relatively stable cyclic performance with minor fluctuations in discharging capacity over six cycles of operation. The first cycle discharge capacity of EDB was 1.65 mAh/cm^2 (at a load resistor of resistance 68 Ω) and charge capacity was 2.00 mAhcm^{-2}, which indicated a coulombic efficiency of 80%. The discharge capacity during the second cycle of operation was 1.64 mAh/cm^2 (decreased by 0.6% than that of the first cycle), while during the sixth cycle of operation, the discharge capacity of the EBD increased and was higher (1.69 mAh/cm^2) than that of all the previous cycles, which indicated that the coulombic efficiency of 84.5% was achieved in the sixth cycle of operation. The minor fluctuation in the discharge capacity of EBD in each cycle test is due to our experimental procedure, which involves

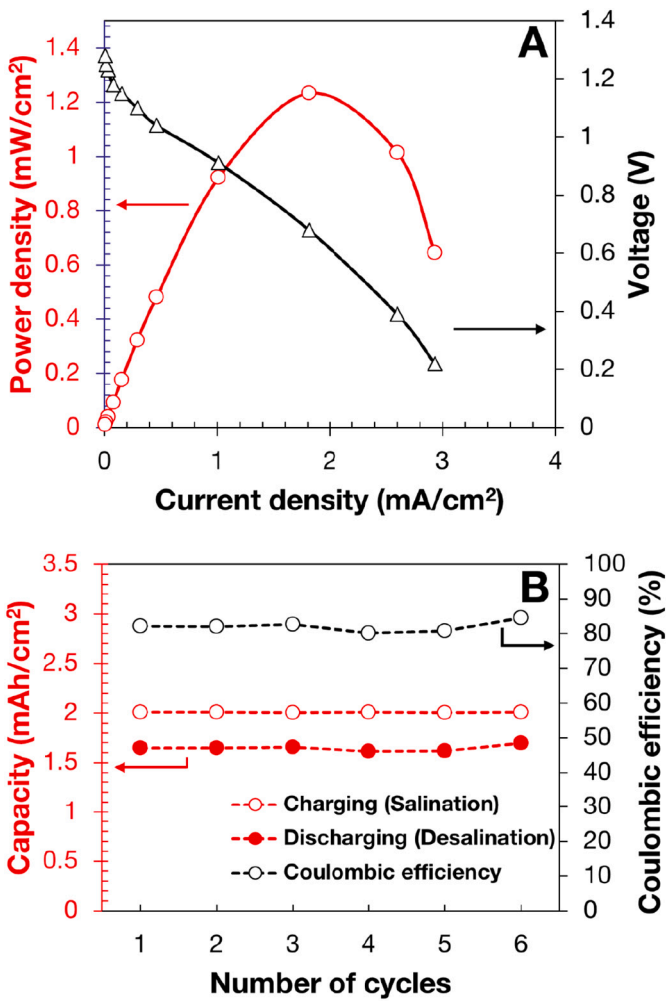

Fig. 5. (A) Polarization curve; and (B) charge-discharge capacity and coulombic efficiency of the EDB for different cycles. Six charging and discharging cycles were operated.

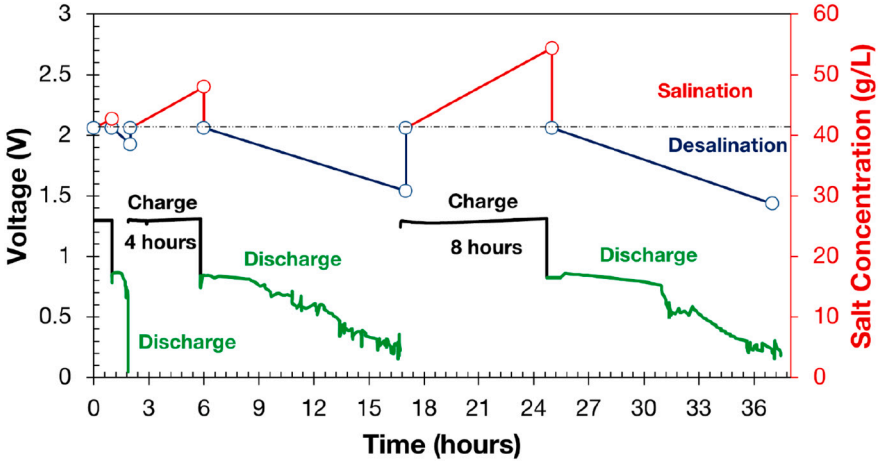

Fig. 4. Variation of salinity and discharge time with different charging periods at a discharge load resistor of 68 Ω.

manually changing the saline water in the desalination chamber. The experiment was performed at room temperature but any fluctuations in temperature can change the conductivity of the saline water in the desalination chamber, consequently, the ohmic resistance of the EBD is changed producing minor fluctuation in discharge capacity. This result is consistent with what has been reported in a previous study in which fluctuation in cell capacity was observed due to experimental procedures [39].

3.3. Effect of saline water volume and charging-discharging time on the performance of EDB

Fig. 6A shows the relationship between the current density produced by the EDB at the different volumes of saline water in the desalination chamber. A linear relationship between the current density and saline water volume was observed when saline water volume was varied between 5 and 20 mL. The maximum current density produced by the EDB during the discharge cycle (discharge was done after charging it for 2 h) at solution saline water volume of 20 ml was 1.56 mA/cm^2. However when the volume of saline water was decreased to 10 ml, then the maximum current density produced by the EDB was decreased to 0.6 mA/cm^2 (62% reduction) and a further decrease in salt volume to 5 mL, decreased the maximum current density to 0.35 mA/cm^2, which is about 80% reduction in current density when compared with that produced by the EDB at saline water volume of 20 ml. The current density in the EDB is driven by the ionic transfer caused by the electron-release, transfer, and electron-acceptance process, which also depends on the volumetric ratio (volume of anode/cathode) and the volume of saline water in the desalination chamber [7]. For a fixed volume desalination chamber, a decrease in the volume of saline water will reduce the liquid-membrane contact cross-sectional area which in turn decreases the rate of ionic flux transport between membranes and anode/cathode chambers and finally resulting in lower current density production. Furthermore, the salination rate of EDB was analyzed by varying the charging period and it was found that the salination rate of EDB during the charging cycle is dependent upon the charge cycle time. Fig. 6B shows the relationship between the salination rate at different periods of the charging step. The salination rate (%) varied following a linear trend with the increase in charging time (hours). About 3.85% of salination rate was observed at charging time of 1 h and when the charging time was increased to 2 h, the salination rate was increased to 7.22%, and increasing charging time to 8 h increased the salination rate to 27.1% (Fig. 6B). Increasing the charging time increases the net electrical energy supplied to the EDB, which drives more Na^+ and Cl^- ions into the middle desalination chamber, thereby producing concentrated brine and thus increase the salination rate. On the other hand, the desalination rate of EDB varied with charging time (Fig. 6C) and a linear relationship was obtained between the desalination rate and the discharge time for discharge times between 1.7 h to 13.4 h (Fig. 6C). The higher was the discharge time, the higher was the desalination rate. For instance, at a discharge time of 1.7 h, the obtained desalination rate was about 5.2%. However, when discharge time was increased to 13.4 h, the desalination rate also increased to 30.3% (Fig. 6C). It should be noted that the discharge time of EDB also dependent on the duration of charging time (Fig. 4). Therefore, to maximize the desalination rate of the EDB, it is necessary to optimize both charging and discharging cycles/times of the EDB. It is also possible that osmotic effect can cause movement of solvent into the desalination chamber thereby decreasing salinity in the middle chamber. Table 2 shows the data for charge and discharge cycles at different desalination chamber volumes with respect to the discharge times. It can be noted that the volume difference before and after (i.e., charging and discharging cycles) the cycles is very small (0.1–0.5 mL or 0.5% to 5%). However, higher discharge time has shown a significant effect of up to 10% salination and desalination, probably due to osmotic effect. In addition, the electrical energy produced by the cell during different discharge cycles at an external resistor of 68 Ω was calculated. Similar to other performance factors, a linear relationship was observed between the discharge period and the energy production rate of the cell. The energy produced by the EDB at 2 h of discharge period was 2.3 mWhr/cm^2. When the discharge period was increased to 13.4 h, the energy

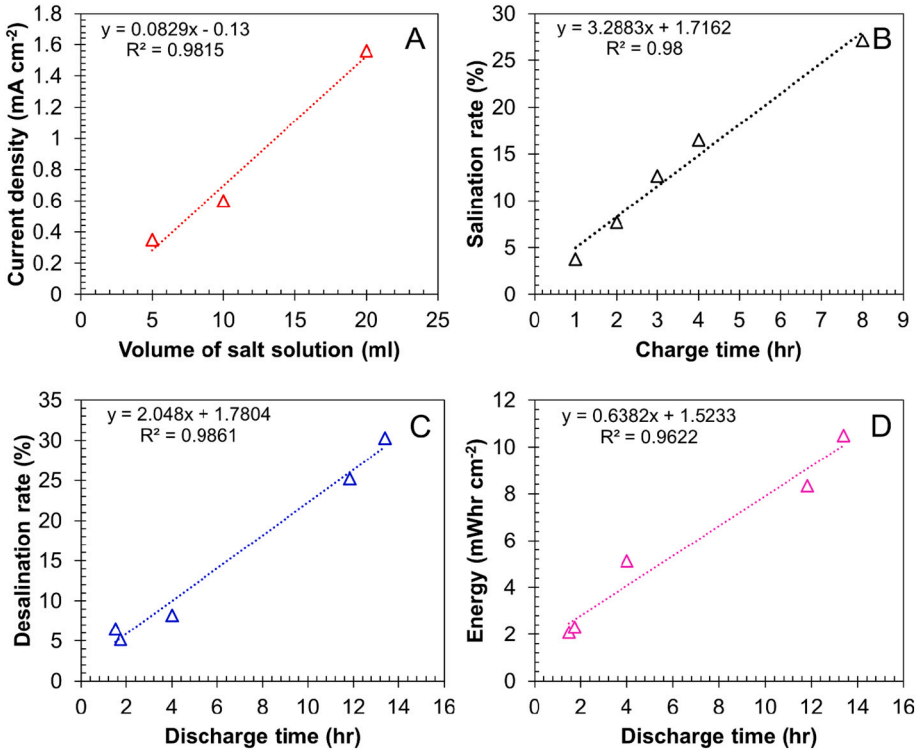

Fig. 6. (A) Correlation between the volume of saline water and the amount of current density produced by EDB; (B) A correlation between salination rate and charge time; (C) A correlation between desalination rate and discharge time; and (D) A correlation between energy generated by EDB and discharge time.

Table 2
Volumetric difference potentially caused by osmotic difference in three different charge-discharge cycles.

Half cycle	Run time (hr)	Initial conc. (g/L)	Final conc. (g/L)	% change conc.	Initial Vol (mL)	Final Vol (mL)	Desal rate (g/L/h)
Charge 1	2.01	39.6	41.2	4.0	20.0	20.3	0.80
Discharge 1	3.99	39.6	36.6	−7.6	20.0	19.9	−0.75
Charge 2	2.00	39.6	42.9	8.3	10.0	10.2	1.65
Discharge 2	9.82	39.6	33.2	−16.2	10.0	9.5	−0.65
Charge 3	2.00	39.6	46.3	16.9	5.00	5.35	3.35
Discharge 3	22.35	39.6	27.7	−30.1	5.00	4.28	−0.53

production rate was increased to 10.5 mWhr/cm^2 (Fig. 6D).

3.4. Desalination performance

To demonstrate the feasibility of the EDB, desalination performance was examined with saline water (0.7 M NaCl; 41.2 g/L) in the desalination chamber. The desalination performance of the EDB was examined with three different charge capacities (2 mAh/cm^2, 8 mAh/cm^2, and 16 mAh/cm^2). At a charge capacity of 2 mAh/cm^2, 7% desalination was observed, however after increasing the charge capacity to 8 mAh cm^{-2}, the desalination rate was increased to 25.2%. Further increase in the charge capacity up to 16 mAh/cm^2, the desalination rate increased to 30.3% (Fig. 7A). Higher charge capacity with fixed charging current density implies a longer charging period and higher desalination rate. It should be noted that the desalination performance depends on the ratio of the charge rate, electrolyte to saline water ratio, and the concentration of electrolytes, which need further consideration through detailed studies. Furthermore, to determine the kinetics of salt removal during the discharging cycle, the concentration of saline water in the desalination chamber was analyzed at each hour of the discharge cycle. (Fig. 7B) shows the discharge voltage profile (at an external resistor of 68 Ω) of the EDB and the concentration of the saline water in the desalination chamber at each hour of the discharge cycle. The results showed that the discharge cycle has lasted for about 6.6 h and the salinity (TDS) decreased linearly with discharge time (Fig. 7B).

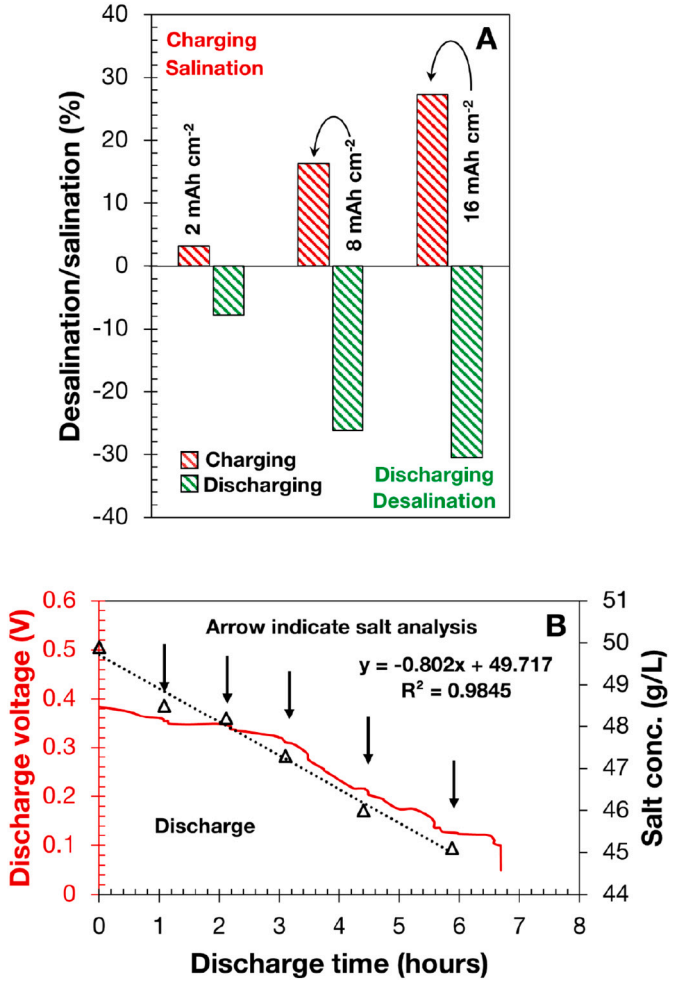

Fig. 7. (A) Desalination/salination rates during charging and discharging periods of the EDB at different charge capacities; (B) Discharge voltage profile and salt concentrations at each hour of the discharge cycle.

3.5. Energy balance

The energy balance of the electrochemical cell was calculated for different charging and discharging cycles. Energy production during discharging and energy consumption during the charging process of the EDB were considered. During the charging process, four charge cycles with 1, 2, 4, and 8 h of charging periods were performed and complete discharge through an external resistor of resistance 68 Ω was performed after each charge cycle. Fig. 8 shows the trends of energy production and consumption by the EDB at different charge periods of 1, 2, 4, and 8 h. The results showed that both energy consumption and production by the EDB increased with charge time (Fig. 8). The energy consumed by the EDB was 2.8 mAh/cm^2, 5.6 mAh/cm^2, 11.2 mAh/cm^2, and 22.4 mAh/cm^2 during charging period of 1 h, 2 h, 4 h, and 8 h, respectively, and the corresponding energy production rates were 2.08 mAh/cm^2, 2.3 mAh/cm^2, 8.34 mAh/cm^2, and 10.5 mAh/cm^2, respectively. In each charge and discharge cycle, the energy consumption was found to be higher than that of energy production. However, in actual desalination applications, energy consumption is the capital index and large quantities of energy are consumed in desalination processes [20,42]. For instance, 2–10 Wh/L of energy is needed for desalination of saline waters using reverse osmosis [2,20,43] and about 3.5 Wh/L of energy is required for the desalination of seawater using ion concentration polarization desalination [32]. In this study, energy is recovered simultaneously with desalination capability, therefore, the energy required for the desalination process should also be considered and added up to the energy recovery portion so that the actual and overall energy balance would be more appealing. Regardless, the function of charging/discharging in the EDB can provide for storage and recovery of excess energy produced in renewable energy-based desalination processes. This is an added convenience and efficiency in terms of enhanced energy production and affordable desalination.

3.6. Comparison with other electrochemical desalination configurations

A comparison of the present study with other studies has been presented in Table 3. The energy efficiency of this system is in agreement with Nam et al. [39] and is higher than those previously reported desalination battery studies as presented in Table 2. The desalination performance in this study was lower than that of previously reported coin type desalination battery [42]. However, the desalination performance was observed to be greater than that of the redox flow electrodes desalination battery [43]. It should be noted that the desalination performance depends on several factors: the ratio of the charge rate,

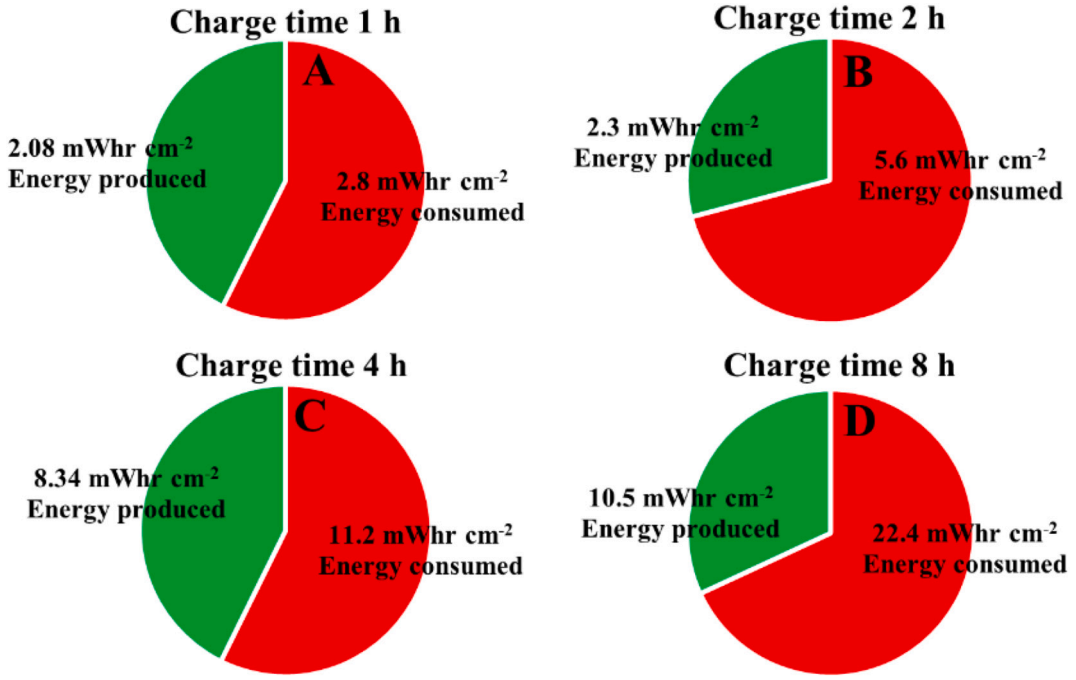

Fig. 8. Energy production and consumption by EDB at the different charging and discharging periods.

Table 3
Comparison of the performance of this study with other studies.

Type	Anolyte	Catholyte	Anode electrode	Cathode electrode	Energy efficiency (%)	CE (%)	Desalination (%)	Reference
Desalination battery $NaTi_2(PO_4)_3$ - Ag	NaCl	NacCl	$NaTi_2(PO_4)_3$	Ag	71.9	99	n/r	[42]
Organic flow desalination battery	FMN-Na[a]	TEMPO[b]	Graphite paper	Graphite paper	25	80	n/r	[46]
Desalination battery $Cu_3[Fe(CN)_6]_2$ as Na-storage	NaCl	NaCl	$Cu_3[Fe(CN)_6]_2$	Bi foam	75.6	97–99.9	n/r	[39]
Coin type	Seawater	Seawater	Carbon	Carbon	63	n/r	77	[44]
Metal-air desalination battery	Simulated seawater	Simulated seawater	Al	Carbon	n/r	n/r	37.8	[47]
Redox flow electrodes desalination battery	$VCl_3 + VCl_2$	NaI	Graphite paper	Graphite paper	50	n/r	~1%	[45]
Silver/silver chloride desalination battery								
$K_3Fe(CN)_6 + K_4Fe(CN)_6{\cdot}3H_2O$ desalination battery	$ZnCl_2$	$K_3Fe(CN)_6 + K_4Fe(CN)_6{\cdot}3H_2O$	Zn	Carbon	74.2	84.5	30.3	This Study

n/r: not reported.
[a] Riboflavin-5′-phosphate sodium salt dehydrate.
[b] 4-Hydroxy-2,2,6,6-tetramethylpiperidin-1-oxyl.

electrolyte to saline water ratio, and the concentration of electrolytes, which needs further consideration through detailed studies.

4. Conclusions

This study demonstrated that an electrochemical battery can be purposely utilized to store electrical energy while simultaneously providing desalination capability by exploiting the charging and discharging processes in the electrochemical cell. While the results obtained from this study are quite encouraging, more detailed investigations should be carried out to study the impact of other electrode and electrolyte combinations for possible improvement in desalination performance. This study showed that the process is suitable for the partial desalination of high saline water. However, it is possible that this method can be conveniently applied to achieve complete desalination of brackish water sources such as groundwater with significant concentrations of total dissolved solids. The storage capacity of the battery is an additional feature that opens up many opportunities for better energy management of grid-independent renewable energy infrastructure suitable for desalination applications.

CRediT authorship contribution statement

Umesh Ghimire: Formal analysis, Investigation, Validation, Writing – review & editing, Data curation, Writing – original draft. **Mary K. Heili:** Investigation, Validation, Writing – review & editing. **Veera Gnaneswar Gude:** Conceptualization, Methodology, Investigation, Writing – review & editing, Supervision, Visualization, Project administration, Funding acquisition.

Declaration of competing interest

The authors declare that they have no known competing financial interests or personal relationships that could have appeared to influence

the work reported in this paper.

Acknowledgments

Mary Heili acknowledges the United States National Science Foundation (NSF) REU Fellowship under the grant, REU-INFEWS 1659830. This research was also supported by the NSF award EAGER 1632019. Any opinions, findings, and conclusions or recommendations expressed in this material are those of the authors and do not necessarily reflect the views of the NSF. Dr. Gude acknowledges the support received from the Kelly Gene Cook, Sr. Endowed Chair in the Richard A Rula School of Civil and Environmental Engineering at Mississippi State University.

Appendix A. Supplementary data

Supplementary data to this article can be found online at https://doi.org/10.1016/j.desal.2020.114929.

References

[1] V.G. Gude, Desalination and sustainability–an appraisal and current perspective, Water Res. 89 (2016) 87–106.
[2] V.G. Gude, V. Fthenakis, Energy efficiency and renewable energy utilization in desalination systems, Prog, Energy, 2020.
[3] H. Lim, Y. Ha, H. Bin Jung, P.S. Jo, H. Yoon, D. Quyen, N. Cho, C.-Y. Yoo, Y. Cho, Energy storage and generation through desalination using flow-electrodes capacitive deionization, J. Ind. Eng. Chem. 81 (2020) 317–322.
[4] V.G. Gude, Desalination and water reuse to address global water scarcity, Rev. Environ. Sci. Bio/Technology. 16 (2017) 591–609.
[5] A.A. Al-Raad, M.M. Hanafiah, A.S. Naje, M.A. Ajeel, Optimized parameters of the electrocoagulation process using a novel reactor with rotating anode for saline water treatment, Environ. Pollut. 265 (2020) 115049.
[6] Y. Feng, L. Yang, J. Liu, B.E. Logan, Electrochemical technologies for wastewater treatment and resource reclamation, Environ. Sci. Water Res. Technol. 2 (2016) 800–831.
[7] U. Ghimire, V.G. Gude, Accomplishing a N-E-W (nutrient-energy-water) synergy in a bioelectrochemical nitritation-anammox process, Sci. Rep. 9 (2019). doi:https://doi.org/10.1038/s41598-019-45620-2.
[8] D. Hlushkou, U. Tallarek, R. Crooks, K. Knust, R. Anand, Electrochemically mediated seawater desalination, Chemie Ing. Tech. 86 (2014) 1447.
[9] S.A. Khalla, M.E. Suss, Desalination via chemical energy: an electrodialysis cell driven by spontaneous electrode reactions, Desalination. 467 (2019) 257–262.
[10] S. Stuart-Dahl, E. Martinez-Guerra, B. Kokabian, V.G. Gude, R. Smith, J. Brooks, Resource recovery from low strength wastewater in a bioelectrochemical desalination process, Eng. Life Sci. 20 (3-4) (2020) 54–66.
[11] M.K. Alsebaeai, T.A. Otitoju, M. bin M.Z. Makhtar, A.L. Ahmad, Membrane distillation: progress in the improvement of dedicated membranes for enhanced hydrophobicity and desalination performance, J. Ind. Eng. Chem. (2020).
[12] I. Phiri, K.Y. Eum, J.W. Kim, W. San Choi, S.H. Kim, J.M. Ko, H. Jung, Simultaneous complementary oil-water separation and water desalination using functionalized woven glass fiber membranes, J. Ind. Eng. Chem. 73 (2019) 78–86.
[13] S. Khodami, S. Mehdipour-Ataei, S. Babanzadeh, Preparation, characterization, and performance evaluation of sepiolite-based nanocomposite membrane for desalination, J. Ind. Eng. Chem. 82 (2020) 164–172.
[14] B. Kokabian, R. Smith, J.P. Brooks, V.G. Gude, Bioelectricity production in photosynthetic microbial desalination cells under different flow configurations, J. Ind. Eng. Chem. 58 (2018) 131–139.
[15] B. Kokabian, U. Ghimire, V.G. Gude, Water deionization with renewable energy production in microalgae-microbial desalination process, Renew. Energy 122 (2018) 354–361.
[16] A. El-Gendi, F.A. Samhan, N. Ismail, L.A.N. El-Dein, Synergistic role of Ag nanoparticles and Cu nanorods dispersed on graphene on membrane desalination and biofouling, J. Ind. Eng. Chem. 65 (2018) 127–136.
[17] M. Peydayesh, T. Mohammadi, O. Bakhtiari, Water desalination via novel positively charged hybrid nanofiltration membranes filled with hyperbranched polyethyleneimine modified MWCNT, J. Ind. Eng. Chem. 69 (2019) 127–140.
[18] O. ul Haq, D.-S. Choi, J.-H. Choi, Y.-S. Lee, Carbon electrodes with ionic functional groups for enhanced capacitive deionization performance, J. Ind. Eng. Chem. 83 (2020) 136–144.
[19] V.G. Gude, N. Nirmalakhandan, S. Deng, Renewable and sustainable approaches for desalination, Renew. Sust. Energ. Rev. 14 (2010) 2641–2654.
[20] V.G. Gude, Energy consumption and recovery in reverse osmosis, Desalin. Water Treat. 36 (2011) 239–260.
[21] F. Calise, F.L. Cappiello, R. Vanoli, M. Vicidomini, Economic assessment of renewable energy systems integrating photovoltaic panels, seawater desalination and water storage, Appl. Energy 253 (2019) 113575.
[22] A. Mollahosseini, A. Abdelrasoul, S. Sheibany, M. Amini, S.K. Salestan, Renewable energy-driven desalination opportunities–a case study, J. Environ. Manag. 239 (2019) 187–197.
[23] V.G. Gude, Energy storage for desalination processes powered by renewable energy and waste heat sources, Appl. Energy 137 (2015) 877–898.
[24] S. Al-Amshawee, M.Y.B.M. Yunus, A.A.M. Azoddein, D.G. Hassell, I.H. Dakhil, H. A. Hasan, Electrodialysis desalination for water and wastewater: a review, Chem. Eng. J. 380 (2020) 122231.
[25] P. Cui, M. Yu, Z. Liu, Z. Zhu, S. Yang, Energy, exergy, and economic (3E) analyses and multi-objective optimization of a cascade absorption refrigeration system for low-grade waste heat recovery, Energy Convers. Manag. 184 (2019) 249–261.
[26] D. Kundu, E. Talaie, V. Duffort, L.F. Nazar, The emerging chemistry of sodium ion batteries for electrochemical energy storage, Angew. Chemie Int. Ed. 54 (2015) 3431–3448.
[27] B. Ok, W. Na, T.-H. Kwon, Y.-W. Kwon, S. Cho, S.M. Hong, A.S. Lee, J.H. Lee, C. M. Koo, Understanding the enhanced electrochemical performance of TEMPO derivatives in non-aqueous lithium ion redox flow batteries, J. Ind. Eng. Chem. 80 (2019) 545–550.
[28] Y.N. Jo, P. Santhoshkumar, K. Prasanna, K. Vediappan, C.W. Lee, Improving self-discharge and anti-corrosion performance of Zn-air batteries using conductive polymer-coated Zn active materials, J. Ind. Eng. Chem. 76 (2019) 396–402.
[29] J.E. Park, M.S. Lim, J.K. Kim, H.J. Choi, Y.-E. Sung, Y.-H. Cho, Optimization of cell components and operating conditions in primary and rechargeable zinc–air battery, J. Ind. Eng. Chem. 69 (2019) 161–170.
[30] D. Desai, E.S. Beh, S. Sahu, V. Vedharathinam, Q. van Overmeere, C.F. de Lannoy, A.P. Jose, A.R. Völkel, J.B. Rivest, Electrochemical desalination of seawater and hypersaline brines with coupled electricity storage, ACS Energy Lett. 3 (2018) 375–379.
[31] W. Tang, J. Liang, D. He, J. Gong, L. Tang, Z. Liu, D. Wang, G. Zeng, Various cell architectures of capacitive deionization: recent advances and future trends, Water Res. 150 (2019) 225–251.
[32] J. Ahn, J. Lee, S. Kim, C. Kim, J. Lee, P.M. Biesheuvel, J. Yoon, High performance electrochemical saline water desalination using silver and silver-chloride electrodes, Desalination. 476 (2020) 114216.
[33] S. Kim, C. Kim, J. Lee, S. Kim, J. Lee, J. Kim, J. Yoon, Hybrid electrochemical desalination system combined with an oxidation process, ACS Sustain. Chem. Eng. 6 (2018) 1620–1626.
[34] M.W. Saleem, B.-G. Im, W.-S. Kim, Electrochemical CDI integration with PRO process for water desalination and energy production: concept, simulation, and performance evaluation, J. Electroanal. Chem. 822 (2018) 134–143.
[35] V. Pothanamkandathil, J. Fortunato, C.A. Gorski, Electrochemical desalination using intercalating electrode materials: A comparison of energy demands, Environ. Sci. Technol. 54 (6) (2020) 3653–3662.
[36] S.J. Kim, S.H. Ko, K.H. Kang, J. Han, Direct seawater desalination by ion concentration polarization, Nat. Nanotechnol. 5 (2010) 297–301.
[37] D.-H. Nam, K.-S. Choi, Electrochemical desalination using Bi/BiOCl electrodialysis cells, ACS Sustain. Chem. Eng. 6 (2018) 15455–15462.
[38] I. Cohen, B. Shapira, E. Avraham, A. Soffer, D. Aurbach, Bromide ions specific removal and recovery by electrochemical desalination, Environ. Sci. Technol. 52 (2018) 6275–6281.
[39] D.-H. Nam, M.A. Lumley, K.-S. Choi, A desalination battery combining Cu3 [Fe (CN) 6] 2 as a Na-storage electrode and Bi as a cl-storage electrode enabling membrane-free desalination, Chem. Mater. 31 (2019) 1460–1468.
[40] J. Luo, B. Hu, C. Debruler, Y. Bi, Y. Zhao, B. Yuan, M. Hu, W. Wu, T.L. Liu, Unprecedented capacity and stability of ammonium ferrocyanide catholyte in pH neutral aqueous redox flow batteries, Joule. 3 (1) (2019 Jan 16) 149–163.
[41] D. Yang, X.Z. Liao, B. Huang, J. Shen, Y.S. He, Z.F. Ma, A Na 4 Fe (CN) 6/NaCl solid solution cathode material with an enhanced electrochemical performance for sodium ion batteries, J. Mater. Chem. A 1 (43) (2013) 13417–13421.
[42] F. Chen, Y. Huang, D. Kong, M. Ding, S. Huang, H.Y. Yang, NaTi2 (PO4) 3-Ag electrodes based desalination battery and energy recovery, FlatChem. 8 (2018) 9–16.
[43] G. Amy, N. Ghaffour, Z. Li, L. Francis, R.V. Linares, T. Missimer, S. Lattemann, Membrane-based seawater desalination: present and future prospects, Desalination. 401 (2017) 16–21.
[44] N. Kim, J.-S. Park, A.M. Harzandi, K. Kishor, M. Ligaray, K.H. Cho, Y. Kim, Compartmentalized desalination and salination by high energy density desalination seawater battery, Desalination. 495 (2020) 114666.
[45] X. Hou, Q. Liang, X. Hu, Y. Zhou, Q. Ru, F. Chen, S. Hu, Coupling desalination and energy storage with redox flow electrodes, Nanoscale. 10 (2018) 12308–12314.
[46] Q. Liang, F. Chen, S. Wang, Q. Ru, Q. He, X. Hou, C. Su, Y. Shi, An organic flow desalination battery, Energy Storage Mater. 20 (2019) 203–207.
[47] M. Ghahari, S. Rashid-Nadimi, H. Bemana, Metal-air desalination battery: concurrent energy generation and water desalination, J. Power Sources 412 (2019) 197–203.